Cessation of rapid late endosomal tubulovesicular trafficking in Niemann–Pick type C1 disease

Mei Zhang*, Nancy K. Dwyer*, Dona C. Love†, Adele Cooney‡, Marcy Comly‡, Edward Neufeld*, Peter G. Pentchev‡, E. Joan Blanchette-Mackie*§, and John A. Hanover†

*Lipid Cell Biology Section and †Cell Biochemistry Section, Laboratory of Cell Biochemistry and Biology, National Institute of Diabetes and Digestive and Kidney Diseases, and ‡Developmental and Metabolic Neurology Branch, National Institute of Neurological Disorders and Stroke, National Institutes of Health, Bethesda, MD 20892

Communicated by G. Gilbert Ashwell, National Institutes of Health, Bethesda, MD, February 12, 2001 (received for review December 13, 2000)

Niemann–Pick type C1 (NPC1) disease results from a defect in the NPC1 protein and is characterized by a pathological accumulation of cholesterol and glycolipids in endocytic organelles. We followed the biosynthesis and trafficking of NPC1 with the use of a functional green fluorescent protein-fused NPC1. Newly synthesized NPC1 is exported from the endoplasmic reticulum and requires transit through the Golgi before it is targeted to late endosomes. NPC1-containing late endosomes then move by a dynamic process involving tubulation and fission, followed by rapid retrograde and anterograde migration along microtubules. Cell fusion studies with normal and mutant NPC1 cells show that exchange of contents between late endosomes and lysosomes depends upon ongoing tubulovesicular late endocytic trafficking. In turn, rapid endosomal tubular movement requires an intact NPC1 sterol-sensing domain and is retarded by an elevated endosomal cholesterol content. We conclude that the neuropathology and cellular lysosomal lipid accumulation in NPC1 disease results, at least in part, from striking defects in late endosomal tubulovesicular trafficking.

Defects of the NPC1 gene cause a severe endocytic accumulation of cholesterol in a variety of cellular and animal models of Niemann–Pick C1 (NPC1) disease (1, 2). The fatal damage in NPC1 disease is neurodegeneration starting from early life. The product of the NPC1 gene (NPC1) is composed of 1,278 aa and is predicted to contain 13 transmembrane domains (2, 3). NPC1 possesses a sterol-sensing domain (SSD) that is also found in two other proteins critical to maintaining cellular cholesterol homeostasis, the sterol response element-binding protein cleavage-activating protein and the enzyme 3-hydroxy-3-methylglutaryl-CoA reductase (2, 4). The cDNA encoding human NPC1 corrects the defect in NPC1 mutant cells and facilitates clearance of the extensive lysosomal pools of cholesterol (2, 5). After biosynthesis of NPC1 in the endoplasmic reticulum, the protein is processed further in the Golgi apparatus (6); at steady state, it is associated with late endosomes. Cellular cholesterol enrichment, through endocytic uptake of low-density lipoprotein (LDL), alters the intracellular distribution of NPC1 protein from a finely dispersed granular pattern to sequestration in prominent cytoplasmic vesicles (7, 8). These NPC1-containing vesicles are positive for lysosomal-associated membrane protein 2 (LAMP2) (7, 9), are not enriched in lysosomal hydrolases (7), and are positive for the late endosomal marker proteins Rab7 (7) and Rab 9 (10). NPC1-containing late endosomes are critical for the retroendocytic trafficking of multiple lysosomal cargo (4, 9). Retroendocytic clearance of fluid phase markers, such as sucrose, from late endosomes is retarded by LDL-derived cellular enrichment of cholesterol (9). We have recently shown that cholesterol modulates glycolipid sorting from NPC1-containing late endosomes into lysosomes (7). In this report, we have visualized functional green fluorescent protein-labeled NPC1 protein (NPC1-GFP) trafficking in living cells. Human NPC1 fibroblasts were also transfected with NPC1-GFP, with similar results reported in this study for CT 60 Chinese hamster ovary (CHO) cells. These studies demonstrate the existence of dynamic late endosomal tubules that affect content exchange among components of the late endocytic compartments, so cells lacking a functional NPC1 protein and cells that accumulate excessive amounts of endocytosed cholesterol show a dramatic dysfunction. Taken together, these findings suggest that the underlying cellular pathology in NPC1 disease results from disordered endocytic tubulovesicular exchange.

Materials and Methods

Cloning of Wild-Type (WT) and Mutant (SSD) NPC1-GFP. The mammalian expression vector for WT human NPC1-GFP, pNES6, was constructed by replacing the stop codon of NPC1 (contained in pSV-SPORT1) (5) with a linker encoding six histidine residues followed by a *Bam*HI site. Between the new *Bam*HI site and the *Not*I site, a fragment encoding GFP from pEGFP-N1 (CLONTECH) was inserted in-frame to create the plasmid pNES6. pNES6-691, encoding GFP-tagged mutant NPC1 (SSD-NPC1-GFP), was constructed by introducing the *Bss*HII/*Not*I fragment from pNES6 into a vector containing the previously described mutant P691S NPC1 cDNA (11). The full-length coding sequences of both vectors were confirmed by DNA sequencing.

Cell Culture and Transfection. WT CHO and mutant CT60 CHO cells that contain the cholesterol lipidosis NPC1 phenotype (12) were maintained in Ham's F-12 medium supplemented with 10% FBS (HyClone). Transfections with mammalian expression vectors encoding NPC1-GFP, SSD-NPC1-GFP (P691S), or GFP were carried out with the use of FuGENE 6 (Roche Molecular Biochemicals), according to the manufacturer's instructions. Briefly, cells were incubated with DNA/FuGENE 6 reagent mixture without serum for 5 h, followed by culturing in 10% FBS-containing medium. For functional analysis of plasmids, cells were fixed, 72 h after transfection, with 3% paraformaldehyde for 30 min and stained with filipin (50 μg/ml) (Polysciences) to assess cholesterol clearance. Twenty-four hours after transfection, cells were incubated with cycloheximide (20 μM) for up to 48 h to assess the duration of NPC1-GFP in the late endosomal compartment and maintenance of cholesterol clearance. Human NPC1 fibroblasts were also transfected with NPC1-GFP, and although the transfection efficiency was low, the results obtained were the same as those derived from transfected CT60 CHO cells, where the transfection efficiency was higher.

Pharmacologic Perturbations. To assess the effect of microtubule disruption on NPC1-GFP trafficking, cells were cultured in 10%

Abbreviations: GFP, green fluorescent protein; NPC1, Niemann–Pick type C1; SSD, sterol-sensing domain; LAMP, lysosomal-associated membrane protein; LDL, low-density lipoprotein; CHO, Chinese hamster ovary; WT, wild type.

§To whom correspondence and reprint requests should be addressed at: Lipid Cell Biology Section, Building 8, Room 427, NINDK, National Institutes of Health, 8 Center Drive, MSC 0850, Bethesda, MD 20892. E-mail: joanbm@bdg8.niddk.nih.gov.

The publication costs of this article were defrayed in part by page charge payment. This article must therefore be hereby marked "*advertisement*" in accordance with 18 U.S.C. §1734 solely to indicate this fact.

www.pnas.org/cgi/doi/10.1073/pnas.081070898

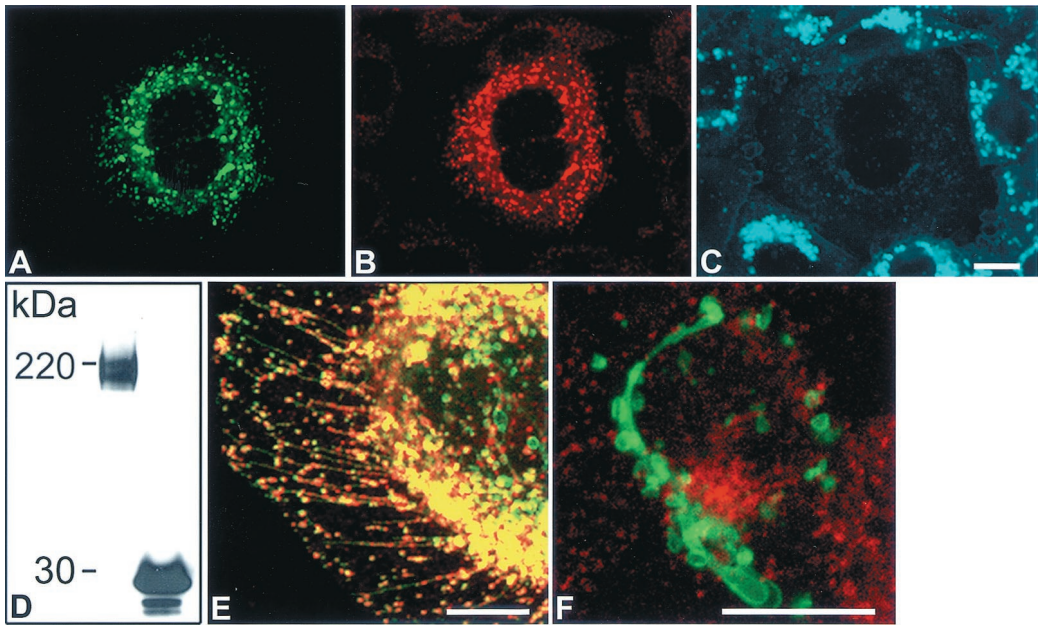

Fig. 1. Expression, functional analysis, and subcellular localization of NPC1-GFP in CT60 CHO cells. (*A*) CT60 CHO cell transfected with NPC1-GFP (green) was (*B*) immunostained with anti-human NPC1 antiserum (red) and (*C*) stained with filipin (blue) to visualize cholesterol-loaded lysosomes. (*D*) Western blot analysis with anti-GFP antibody of total solubilized protein from NPC1-GFP-expressing (*Left*) and EGFP-expressing (*Right*) WT CHO cells. The predicted molecular mass of GFP (27 kDa) combined with glycosylated NPC1 (170 kDa and 190 kDa) is comparable to the 200- and 220-kDa bands. Identical results were obtained with total soluble protein from NPC1-GFP transfected CT60 CHO cells (data not shown). (*E*) Merged image of CT60 CHO cell transfected with NPC1-GFP (green) and immunostained with LAMP2 (red). Colocalization is represented by yellow. (*F*) Merged image of a NPC1-GFP-expressing WT CHO cell. Cells were transfected with NPC1-GFP (green) and pulsed with Texas Red–transferrin (red) for 10 min. *A–C, E,* and *F* are confocal images. (Bar = 10 μm.)

FBS-containing medium with 10 μM nocodazole (Sigma) for up to 2 h at 37°C. To assess the effect of Golgi disruption on NPC1-GFP trafficking WT CHO cells were incubated for 12 h with 10 μM Brefeldin A (Sigma) (13), 17 h after transfection. To assess the effect of cholesterol accumulation on NPC1-GFP trafficking, WT CHO cells were incubated with 10 μg/ml progesterone for 24 h, plus or minus human LDL (100 μg/ml) (14), 48 h after transfection. For long-term depletion of cholesterol, transfected and nontransfected WT CHO and CT60 CHO cells were cultured in 2% lipoprotein-deficient serum for 3–5 days before fusion experiments and imaging.

Endocytosis Assay. Endocytosis was assayed with the use of fluorescent dextran or fluorescent transferrin. To label late endocytic compartments (15), nontransfected cells and cells transfected for 48 h were cultured at 37°C in medium containing 1 mg/ml rhodamine-dextran or fluorescein-dextran (molecular weight 70,000; Molecular Probes) for 12 h followed by washout for 2–12 h before fixation. To label early endocytic compartments (16), cells were cultured at 37°C in medium containing 100 μg/ml Texas Red-transferrin (Molecular Probes) for 10 min before fixation.

Somatic Cell Fusion. Cells were cultured with rhodamine-dextran or fluorescein-dextran, separately, for 12 h followed by chase for 2 h to mark the late endocytic compartments. Prelabeled cells were cocultured in 2-well Lab-Tek chambered cover glasses for 24 h to achieve a confluent monolayer. Cells were washed with Hanks' balanced salt solution three times and fused with 0.5 ml 40% polyethylene glycol 1500 (Roche Molecular Biochemicals) for 1 min 45 s, followed by the addition of 42% polyethylene glycol solution for 1 min 45 s at room temperature. Cells were then washed quickly three times with Hanks' balanced salt solution to remove polyethylene glycol and incubated with 2 ml Ham's F-12 medium, plus or minus FBS, for various times (10, 30, 60 min, 2, 12, 24, 48 h) before fixation and imaging.

Immunoblot Analysis. Forty-eight hours after transfection, cells were lysed in lysis buffer [100 mM Tris·HCl (pH 8.0)/1% Nonidet P-40/150 mM NaCl/0.02% sodium azide/100 mg/ml PMSF/1 μg/ml aprotinin] at 4°C. Extract was centrifuged at 10,000 $\times$ *g* for 3 min at 4°C, and the supernatant was aliquoted and stored at −70°C. Total protein extract from each sample was separated with 6–12% gradient SDS-PAGE. The proteins were transferred to nitrocellulose membrane (NOVEX, San Diego), and Western blot analysis was performed with an enhanced chemiluminescence Western blot kit (Amersham Pharmacia) according to the manufacturer's instructions. The mouse monoclonal antibody against GFP (Roche Molecular Biochemicals) was used at a 1:500 dilution to detect the chimeras. Blots were exposed on Hyperfilm enhanced chemiluminescence (Amersham Pharmacia).

Immunostaining. Cells were fixed with 3% paraformaldehyde in PBS for 30 min to 1 h, washed in PBS, and immunostained with rabbit anti-NPC1 antiserum (7, 9), mouse IgG against CHO LAMP1 and CHO LAMP2 (UH1 and UH3) (monoclonal antibodies were obtained from the Developmental Studies Hybridoma Bank developed under the auspices of the National Institute of Child Health and Human Development and maintained by the Department of Biological Sciences, University of Iowa, Iowa City), and monoclonal IgG against α-tubulin (clone DM1A; Sigma).

Fluorescence Microscopy and Time-Lapse Image Processing. Differential interference contrast images, confocal images, and time-lapse confocal scanning images were obtained with a Zeiss LSM410 confocal microscope system equipped with a krypton-argon Omnichrome laser with excitation wavelengths of 488 nm

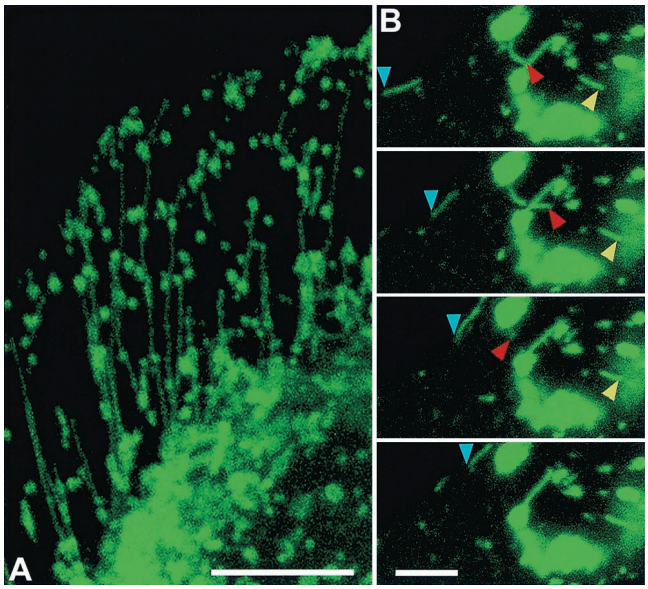

Fig. 2. NPC1-GFP traffic via late endosomal tubules in CHO cells. (*A*) CT60 CHO cells expressing NPC1-GFP (green) were fixed and visualized by confocal microscopy (the cell shown is the one in Fig. 1 *E*). (*B*) Live-cell, confocal-scanning time sequence of NPC1-GFP-containing tubules, showing rapid motion of three NPC1-GFP tubules with variable rates. Blue arrowheads mark tubular trafficking along the periphery of the cell. Red arrowheads mark tubular extension and retraction. Yellow arrowheads mark tubular trafficking among vesicles. The time interval between images is 2 s. All images are confocal. [Bar = 10 μm (*A*) or 5 μm (*B*).] View dynamics of late endosomal tubular trafficking of NPC-1 GFP in Movies 1 and 2.

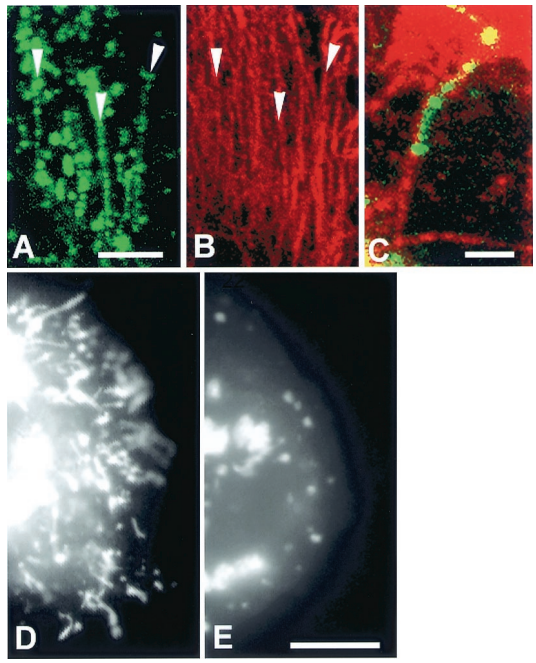

Fig. 3. NPC1-GFP-containing late endosomal tubular trafficking is microtubule dependent. (*A–E*) CT60 CHO cells transfected with NPC1-GFP. Confocal images of fixed cells show NPC1-GFP tubules (*A*, green) aligned along microtubules (*B*, labeled with anti-α-tubulin, red). Arrowheads in *A* and *B* indicate areas of obvious alignment. (*C*) A merged image shows a NPC1-GFP tubule (green) aligned along a microtubule (red). (*D* and *E*) Digital images of living CT60 CHO cells. (*D*) A CT60 CHO cell cleared of cholesterol contains many NPC1-GFP-containing late endosomal tubules. (*E*) A CT60 cell incubated with nocodazole for 70 min. NPC1-GFP-containing late endosomal tubules are not present in cells in which microtubules are depolymerized by nocodazole treatment. *A–C* are confocal images, *D* and *E* are digital epifluorescence images. [Bar = 10 μm (*A* and *B*), 2 μm (*C*), and 10 μm (*D* and *E*).]

and 568 nm for fluorescein and rhodamine, respectively (Zeiss). Filipin fluorescence was viewed with an argon ion laser (Coherent Radiation, Palo Alto, CA) at an excitation wavelength of 351 nm. Time-lapse images were also taken with a Zeiss Axiovert 35 microscope equipped with a charged-coupled device camera (TEA/CCD-1317K/1; Princeton Instruments, Trenton, NJ). For live cell imaging cells were prepared on 40-mm coverslips, and the temperature was maintained at 37°C in a Focht Chamber System 2 with an Objective Heater System (Bioptechs, Butler, PA). Image capture, animation, export to QUICKTIME MOVIE, and calculation of rate of movement of fluorescent structures were performed with the IPLAB software system (Scanalytics, Billerica, MA). To view dynamics of tubular trafficking, see Movies 1–4, which are published as supplemental data on the PNAS web site, www.pnas.org. After live imaging cells were fixed and stained with filipin to assess cellular cholesterol levels.

Results

NPC1 Trafficking Is Mediated by Late Endosomal Tubules Moving Along Microtubules. Trafficking of NPC1 in living cells was examined with fully functional chimeric protein consisting of enhanced *Aequorea victoria* GFP with NPC1 (Fig. 1). Introduction of NPC1-GFP into an NPC1 mutant CHO cell line, CT60 (12), resulted in clearance of accumulated cholesterol (Fig. 1*C*). The expressed protein was intact, as evidenced by immunoblot analysis (Fig. 1*D*). The localization of NPC1-GFP (Fig. 1*A*) in the late endocytic compartment was confirmed by immunolabeling with antibodies to NPC1 (Fig. 1*B*), lysosomal LAMP2 glycoprotein (Fig. 1*E*), and endocytosed dextrans (below). The NPC1-containing late endosomes are distinct from transferrin-containing early endosomes (Fig. 1*F*). NPC1-GFP is capable of maintaining cholesterol clearance in the late endocytic compartments for at least 48 h as assessed by cyclohexamide treatment (*Materials and Methods*). The most striking morphological feature of the NPC1-containing late endosomes, visualized initially in living cells, is the dynamic movement of tubular extensions radiating from late endocytic vesicles (Fig. 2*A*). The NPC1-containing tubules are LAMP2 positive (Fig. 1*E*). Formation of the tubules and their rapid motion were monitored with time-lapse imaging (Fig. 2*B* and Movies 1 and 2). Tubules, extending from vesicles and traveling at fast rates of 1–5 μm/s, merge with other vesicles. Most of the NPC1-containing tubules move bidirectionally, between perinuclear vesicles near the microtubule organizing center and the cell surface (Fig. 2*A*), and are aligned along microtubules (Fig. 3 *A–C*). Consistent with this observation was the finding that treatment of living cells with nocodazole to disrupt microtubules (17) resulted in inhibition of NPC1-containing tubular trafficking (Fig. 3*E*). Within 9 min of nocodazole treatment, the few tubules that remained extended from late endocytic vesicles and did not appear to travel or merge with other vesicles. Longer treatment with nocodazole totally blocked late endosomal tubule formation and resulted in NPC1-containing vesicles being clumped in the perinuclear microtubule organizing center of the cell (Fig. 3*E*). Rapid, constitutive, late endosomal tubular trafficking along microtubules would result in efficient exchange of membrane and fluid phase molecules within the endocytic pathway.

Translocation of NPC1-GFP from Site of Synthesis in Endoplasmic Reticulum to Late Endosomes Is Dependent upon Golgi Function. NPC1 protein synthesized in the endoplasmic reticulum moves to the Golgi apparatus for processing of its N-linked oligosaccharides (6). Our study on living cells shows an accumulation of NPC1-GFP in the endoplasmic reticulum network within 12 h after transfection;

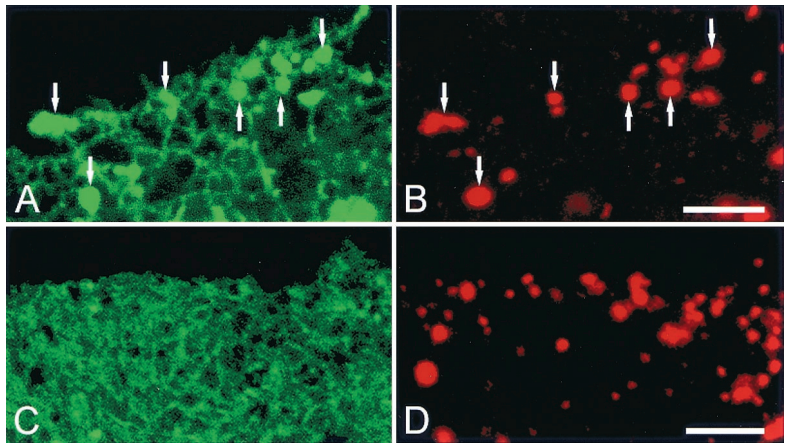

Fig. 4. Endosomal accumulation of newly synthesized NPC1-GFP is prevented by disruption of the Golgi apparatus by treatment with Brefeldin A. CT60 CHO cells transfected with NPC1-GFP contain the protein in endoplasmic reticulum (*A*) and in late endosomal vesicles (*A*, arrows) that contain rhodamine-dextran (*B*, arrows). In Brefeldin A–treated cells NPC1-GFP is present in the endoplasmic reticulum (*C*) but not in rhodamine-dextran labeled late endosomes (*D*). All images are confocal. (Bars = 5 μm.)

NPC1-GFP then appears in tiny vesicles dispersed among cisternal elements of the endoplasmic reticulum within 17 h of transfection (Fig. 4*A*). These early NPC1-GFP-containing vesicles are identified as late endosomes because they contain endocytosed fluorescent dextran (Fig. 4*B*) (15). In cells treated with Brefeldin A, to block Golgi-bound vesicles from leaving the endoplasmic reticulum (13, 18), NPC1-GFP is present in the endoplasmic reticulum (Fig. 4*C*) but not in fluorescent dextran-loaded late endosomes (Fig. 4 *B* and *D*). This finding suggests that NPC1-GFP must first move through the Golgi apparatus to reach late endosomes and argues against direct interaction between late endosomes and the endoplasmic reticulum. In transiently transfected CHO cells, NPC1-GFP clears from the endoplasmic reticulum after 24 h and resides in late endosomal vesicles and their dynamic tubular extensions for up to 5 days.

Late Endosomal Tubular Trafficking Is Modulated by Cholesterol Content. Intracellular sterol levels affect the tubular trafficking of NPC1-containing late endosomes. CT60 CHO cells, transfected with wtNPC1-GFP for 24–48 h, contain NPC1-GFP (Fig. 5*B*) at the periphery of cholesterol-laden lysosomes (Fig. 5 *A* and *C*) and in long, curved, immobile tubules (Fig. 5*C*). When NPC1 subsequently affects clearance of cholesterol from mutant cells (Fig. 5*D*), dynamic NPC1-GFP-containing late endosomal tubular trafficking is restored (Fig. 5*E*). Cholesterol inhibition of late endosomal tubular trafficking is also seen in CT60 CHO cells transfected with GFP-labeled SSD-NPC1 (Fig. 6*A*), a mutant construct that is unable to clear cholesterol (Fig. 6*B*). SSD-NPC1-GFP locates to the periphery of cholesterol-laden lysosomes (Fig. 6*C*) and in long, curved, nonmobile late endocytic tubules (not shown) that are labeled by NPC1 immunostaining (Fig. 6*D*) and endocytic uptake of rhodamine-dextran (Fig. 6*E*). These transfected CT60 CHO cells do not clear cholesterol with time, and SSD-NPC1-GFP-containing late endosomal tubules remain immobile. In contrast, SSD-NPC1-GFP traffics rapidly in the dynamic late endosomal tubules of WT CHO cells. In WT CHO cells transfected with wtNPC1-GFP but incubated with progesterone and LDL to induce cholesterol accumulation (14), NPC1-GFP is located at the periphery of cholesterol-laden lysosomes and in straight, rigid, late endosomal tubules that show no motion in time-lapse videos (Movies 3 and 4). Upon removal of progesterone and clearance of cholesterol (14), late endocytic tubules become flexible and exhibit dynamic motion (data not shown). Progesterone treatment without LDL uptake does not alter late endosomal trafficking in CHO cells (data not shown). These findings show that late endosomal tubular trafficking is cholesterol dependent and that maintenance of cholesterol levels by NPC1 is essential for tubular mobility.

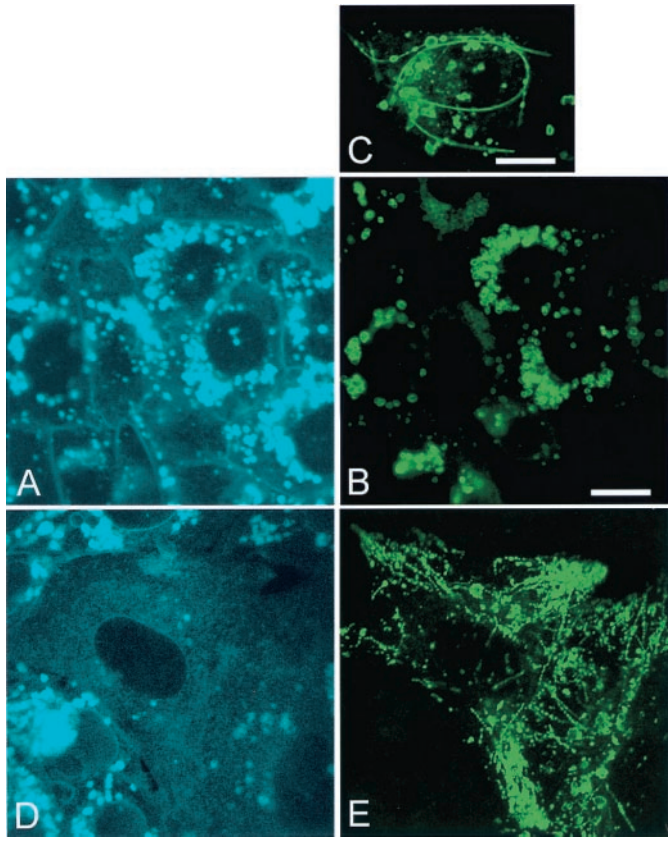

Fig. 5. Clearance of cholesterol in CT60 CHO cells by NPC1-GFP restores late endosomal tubular trafficking. (*A–C*) CT60 CHO cells transfected with NPC1-GFP (48 h) but not yet cleared of lysosomal cholesterol (*A*). In cholesterol-laden cells NPC1-GFP (*B*) locates to the surface of lysosomes (*B* and *C*) and in long nonmobile late endosomal tubules (*C*). (*D* and *E*) CT60 CHO cells transfected with NPC1-GFP (72 h) and cleared of cholesterol. Cholesterol clearance (*D*) reestablishes late endosomal tubular trafficking (*E*). All images are confocal. (Bars = 10 μm.) View nonmobile late endosomal tubules containing NPC-1 GFP or rhodamine-dextran in Movies 3 and 4.

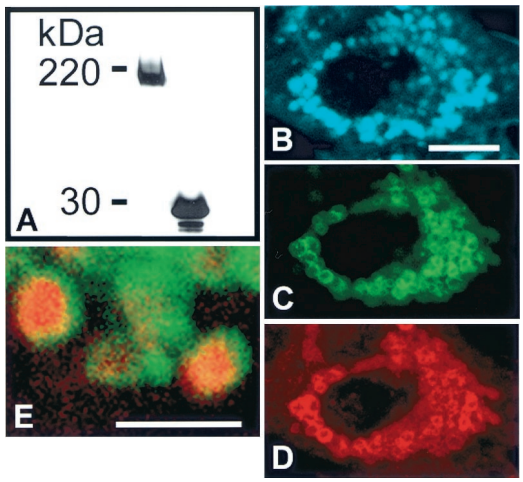

Fig. 6. Late endocytic trafficking is blocked by cholesterol accumulation in CT60 CHO cells expressing SSD-NPC1-GFP. (*A*) Western blot analysis with anti-GFP antibody of total solubilized protein from SSD-NPC1-GFP-expressing WT CHO cells (*Left*) and EGFP-expressing WT CHO cells (*Right*). The predicted molecular mass of GFP (27 kDa) combined with glycosylated SSD-NPC1 (170 kDa) is comparable to the 200-kDa band (*Left*). (*B–E*) CT 60 CHO cells expressing SSD-NPC1-GFP fail to clear cholesterol. Seventy-two hours after transfection, cells were fixed, stained, and labeled with filipin (*B*, blue) to visualize cholesterol by confocal microscopy. SSD-NPC1-GFP (*C*, green) was also detected by indirect immunofluorescence (*D*, red). (*E*) Cholesterol-laden lysosomes in an SSD-NPC1-GFP transfected CT60 CHO cell are labeled by endocytic uptake of rhodamine-dextran. In this merged image, SSD-NPC1-GFP (green) is present as rings at the periphery of rhodamine-dextran (red) in the cholesterol-laden core of lysosomes. *B–E* are confocal images. [Bar = 10 μm (*B–D*) and 2 μm (*E*).]

Content Exchange Among Late Endocytic Compartments Is Facilitated by NPC1 via Clearing of Cholesterol. The dramatic alterations in tubulovesicular motion of NPC1-containing endosomes might be associated with a corresponding change in endosomal content. To test this hypothesis WT CHO and CT60 CHO cells were incubated with fluorescent dextrans to prelabel late endocytic NPC1-containing compartments before somatic cell fusion (19, 20). CT60 CHO cells cultured in LDL-containing medium were labeled with either individual rhodamine-dextran or fluorescein-dextran for 24 h and then fused. Cell fusion was confirmed by differential interference contrast microscopy to identify multinucleated cells (Fig. 7*A*). These fused cells were laden with cholesterol (Fig. 7*B*). The lysosomes in fused cells contained either rhodamine-dextran or fluorescein-dextran, showing that there was little mixing of lysosomal contents, via late endosomal trafficking, in these cholesterol-laden cells for up to 48 h after fusion (Fig. 7 *C–E*). CT60 CHO cells were partially depleted of cholesterol by incubation in lipoprotein-deficient serum for 5 days and then incubated with either rhodamine-dextran or fluorescein-dextran for 24 h and fused (Fig. 7*F*). In the cholesterol-depleted, fused CT60 CHO cells (Fig. 7*G*) dextran is rapidly exchanged between late endocytic compartments as early as 2 h after fusion. Late endocytic compartments in the fused cells contain both rhodamine-dextran and fluorescein-dextran (Fig. 7 *H–J*). This content exchange is accompanied by redistribution of NPC1-GFP within the late endocytic compartment and is retarded by nocodazole treatment (data not shown). Fusion between dextran-labeled WT CHO cells demonstrated rapid exchange (within 2 h) between late endocytic compartments, which is consistent with reported studies (19, 20). However, fusion between WT CHO and CT60 CHO cells showed that content exchange between late endocytic compartments was present only when the fused cells were

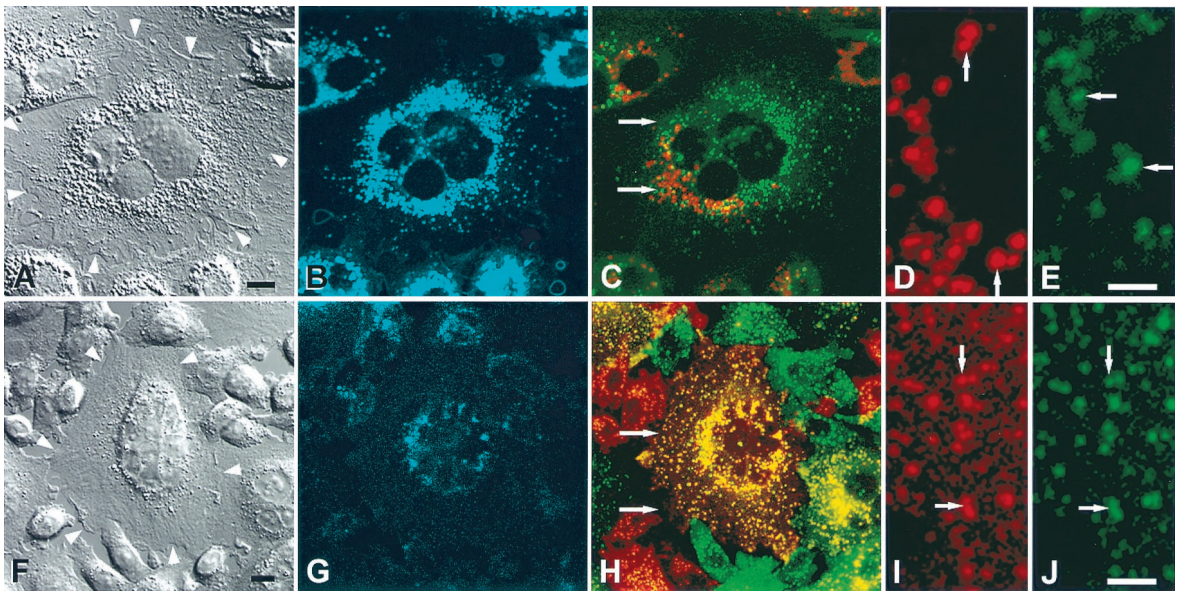

Fig. 7. Cholesterol accumulation impedes communication between late endocytic compartments in fused CT60 CHO cells. CT60 CHO cells cultured in 10% FBS (*A–E*) or in lipoprotein-deficient serum to partially deplete lysosomal cholesterol (*F–J*) were incubated with fluorescein-dextran or rhodamine-dextran, then fused (see *Materials and Methods*). Cells were fixed and examined by confocal microscopy. (*A*) A differential interference contrast image shows a fused cell with four nuclei, prominent lysosomes in the center of the cell, and cell boundaries (white arrowheads). (*B*) Lysosomes are loaded with cholesterol (blue). (*C*) Merging of rhodamine and fluorescein images of a fused cell shows that lysosomes contain either rhodamine-dextran (red) or fluorescein-dextran (green). The rhodamine-dextran-containing lysosomes are separate from the fluorescein-dextran-containing lysosomes (indicated by green and red). (*D* and *E*) Separate red and green images at higher magnification of area delineated by white arrows in *C*. Rhodamine-dextran-containing lysosomes (*D*, arrows) are not visible in *E*. Green dextran-containing lysosomes (*E*, arrows) are not visible in *D*. (*F*) Differential interference contrast image shows a fused cell with four nuclei, a few central lysosomes, and cell boundaries (white arrowheads). (*G*) Lysosomes in the center of the cell contain little cholesterol (blue). (*H*) Merging of rhodamine and fluorescein images of a fused cell shows that lysosomes and late endosomes contain both rhodamine-dextran and fluorescein-dextran (yellow). (*I* and *J*) Separate red and green images at higher magnification of area delineated by white arrows in *H*. Rhodamine-dextran-containing late endosomes and lysosomes (*I*, red at arrows) colocalize with fluorescein-dextran-containing late endosomes and lysosomes (*J*, green at arrows). *B–E* and *G–J* are confocal images. [Bar = 10 μm (*A, B, F–H*) and 5 μm (*E, D, J, I*).]

cleared of cholesterol (data not shown). We conclude that NPC1 mutant cells do not efficiently perform endocytic mixing because of cholesterol accumulation, which results in inhibition of late endosomal tubular trafficking.

Discussion

We have demonstrated that trafficking of the NPC1 protein occurs along a late endosomal tubular reticulum sensitive to cellular cholesterol load derived from uptake of LDLs. Endocytosed cell surface receptors and their ligands enter an early tubular endosomal pathway that sorts ligand–receptor complexes recycling to the plasma membrane from others destined to travel through the later arm of the endosomal pathway (21). Endocytic uptake of LDL recruits NPC1 protein into a Rab 7 positive late endosomal compartment (7). NPC1-GFP is visualized to be trafficking in living cells between late endosomal compartments and lysosomes, via an extensive system of branching tubules with rapid rates of movement in the range of 1–5 μm/s. In normal cells, under physiological conditions, cholesterol homeostasis is maintained, and cholesterol is so efficiently retrieved from early compartments of the endocytic pathway that it does not gain access to lysosomes.

The role of the NPC1 protein in maintaining basal cellular cholesterol concentrations within the endosomal reticulum is well established by the phenotype presentation of the NPC1 mutation, because in mutant cells LDL cholesterol accumulates in lysosomes. Strikingly this overload of cellular cholesterol affects the structure and mobility of late endosomal tubules. Cholesterol inhibition of late endosomal tubular trafficking was visualized in living, cholesterol-loaded WT CHO cells (incubated with LDL + progesterone and expressing WT NPC1-GFP) and mutant CT60 CHO cells (expressing nonfunctional mutant NPC1-GFP). When egress of cholesterol from WT CHO cells is accomplished by washout of progesterone and from CT60 CHO cells by extended incubation in lipoprotein-deficient serum or expression of functional NPC1-GFP, late endosomal tubular trafficking is reestablished. NPC1 has several membrane-spanning regions (2, 3) that predict its residence in the membrane boundaries of the endocytic pathway. Cholesterol affects the rigidity of membranes (22), which may result in the elongated, straight, nonmobile endosomal tubules present in cholesterol-loaded cells and perhaps inhibits scission of vesicles normally budding from endosomal tubules (23). We have shown that NPC1-dependent sorting of lipids occurs within the late endosomal compartment, achieving selective distribution of glycolipids between late endosomes and cholesterol-loaded lysosomes (7).

We conclude that the NPC1 protein plays a pivotal role in the endosomal tubular reticulum, regulating both lipid sorting and tubular trafficking. One may consider that as cholesterol enters late endocytic tubules, recruitment of NPC1 protein efficiently maintains retrograde cholesterol transport to the plasma membrane until a set point is reached, beyond which cholesterol overload is then sorted to lysosomes and accumulates in this late storage compartment of the endocytic pathway. The NPC1 protein would function to maintain a basal concentration of cholesterol in endosomal membranes, compatible with cellular needs and endosomal tubular mobility. How NPC1 effects cholesterol clearance is not yet known. Bacterially expressed NPC1's permease activity effects the transport of fatty acids, but not cholesterol, across membranes (24), suggesting that cholesterol transport may occur via trafficking within membranes of endocytic compartments. Because NPC1 is a transmembrane protein containing a SSD, NPC1 may interact with cholesterol-rich domains in late endosomal membranes to facilitate cholesterol flow within leaflets of membrane bilayers.

Our demonstration that movement of late endosomal tubules is microtubule-based may have important implications for understanding NPC1 disease. The cholesterol-induced cessation of microtubule-based movement might be expected to have a particularly dramatic effect on neuronal function. The neuron is known to be highly dependent upon microtubules for axonal transport, and it is likely that endosomal movement along the microtubule conduit is critical for neuronal cell viability. This observation provides an important clue to understanding the various pathogenic features of NPC1 disease, which includes neuronal cell death in humans and other species.

Maintenance of the endosomal–lysosomal system as a dynamic and pleomorphic reticulum plays a key role in cell function. Trafficking of lipids within the reticulum and modulation of local lipid concentrations by NPC1 protein could be a normal physiological response to LDL uptake. The result of mutant, nonfunctional NPC1 protein is lipid imbalance within the endosomal reticulum and a shift of cholesterol and selected glycolipids to the storage lysosomal compartment. The consequences of abnormal cellular lysosomal storage, such as neuronal degeneration and pathological accumulation of extracellular debris are known to occur in many inherited storage disorders, including NPC1 disease (1, 25).

1. Patterson, M. C., Vanier, M., Suzuki, K. Morris, J., Carstea, E., Neufeld, E. B., Blanchette-Mackie, E. J. & Pentchev, P. G. (2000) in *The Metabolic and Molecular Basis of Inherited Diseases*, 8th Ed. (McGraw–Hill, New York).
2. Carstea, E. D., Morris, J. A., Coleman, K. G., Loftus, S. K., Zhang, D., Cummings, C., Gu, J., Rosenfeld, M. A., Pavan, W. J., Krizman, D. B., *et al.* (1997) *Science* **277,** 228–231.
3. Davies, J. P. & Ioannou, Y. A. (2000) *J. Biol. Chem.* **275,** 24367–24374.
4. Blanchette-Mackie, E. J. (2000) *Biochim. Biophys. Acta* **1486,** 171–183.
5. Watari, H., Blanchette-Mackie, E. J., Dwyer, N. K., Glick, J. M., Patel, S., Neufeld, E. B., Brady, R. O., Pentchev, P. G. & Strauss, J. F., 3rd (1999) *Proc. Natl. Acad. Sci. USA* **96,** 805–810.
6. Watari, H., Blanchette-Mackie, E. J., Dwyer, N. K., Sun, G., Glick, J. M., Patel, S., Neufeld, E. B., Pentchev, P. G. & Strauss, J. F., 3rd (2000) *Exp. Cell. Res.* **255,** 56–66.
7. Zhang, M., Dwyer, N. K., Neufeld, E. B., Love, D. C., Cooney, A. M., Comly, M., Patel, S., Watari, H., Strauss, J. F., 3rd, Pentchev, P. G., *et al.* (2001) *J. Biol. Chem.* **276,** 3417–3425.
8. Puri, V., Watanabe, R., Dominguez, M., Sun, X., Wheatly, C., Marks, D. & Pagano, R. (1999) *Nat. Cell Biol.* **1,** 386–388.
9. Neufeld, E.B., Wastney, M., Patel, S., Suresh, S., Cooney, A. M., Dwyer, N. K., Roff C. F., Ohno, K., Morris, J. A., Carstea, E. D., *et al.* (1999) *J. Biol. Chem.* **274,** 9627–9635.
10. Higgins, M. E., Davies, J. P., Chen, F. W. & Ioannou, Y. A. (1999) *Mol. Genet. Metab.* **68,** 1–13.
11. Watari, H., Blanchette-Mackie, E. J., Dwyer, N. K., Watari, M., Neufeld, E. B., Patel, S., Pentchev, P. G. & Strauss, J. F., 3rd (1999) *J. Biol. Chem.* **274,** 21861–21866.
12. Cruz, J. C., Sugii, S., Yu, C. & Chang, T.-Y. (2000) *J. Biol. Chem.* **275,** 4013–4021.
13. Lippincott-Schwartz, J., Glickman, J., Donaldson, J. G., Robbins, J., Kreis, T., E., Seamon, K. B., Sheetz, M. P. & Klausner, R. D. (1991) *J. Cell Biol.* **112,** 567–577.
14. Butler, J. D., Blanchette-Mackie, E. J., Goldin, E., O'Neill, R. R., Carstea G., Roff, C. F., Patterson, M. C., Patel, S. C., Comly, M. E., Cooney, A., *et al.* (1992) *J. Biol. Chem.* **267,** 23797–23805.
15. Chen, C. S., Bach, G. & Pagano, R. E. (1998) *Proc. Natl. Acad. Sci. USA* **95,** 6373–6378.
16. Hopkins, C. R., Gibson, A., Shipman, M. & Miller, K. (1990) *Nature (London)* **346,** 335–339.
17. Hoebeke, J., Van Nijen, G. & De Brabander, M. (1976) *Biochem. Biophys. Res. Commun.* **69,** 319–324.
18. Rambourg, A., Clermont, Y., Jackson, C. L. & Kepes, F. (1995) *Anat. Rec.* **241,** 1–9.
19. Ferris, A. L., Brown, J. C., Park, R. D. & Storrie, B. (1987) *J. Cell Biol.* **105,** 2703–2712.
20. Deng, Y. P. & Storrie, B. (1988) *Proc. Natl. Acad. Sci. USA* **85,** 3860–3864.
21. Hopkins, C. R. (1983) *Cell* **35,** 321–330.
22. Stryer, L. (1995) in *Biochemistry* (Freeman, New York), 4th Ed., pp. 279–280.
23. Dobereiner, H. G., Kas, J., Noppl, D., Sprenger, I. & Sackmann, E. (1993) *Biophys. J.* **65,** 1396–1403.
24. Davies, J. P., Chen, F. W. & Ioannou, Y. A. (2000) *Science* **290,** 2295–2298.
25. Cataldo, A. M., Hamilton, D. J., Barnett, J. L., Paskevitch, P. A. & Nixon, R. A. (1996) *J. Neurosci.* **16,** 186–199.